VIBRATION ANALYSIS OF ROTARY DRIER

František Palčák*, Martin Vančo*

In this paper the transfer of vibration from motor to the bottom group of rotary drier is analyzed in the ADAMS/Vibration module environment. Excitation from unbalanced motor shaft is transferred through bearings mounted in side shields to the transmission device and bottom plate. Output results were time-domain courses of displacement, velocity, acceleration and transfer functions, frequency response functions and modal coordinates corresponding to excitation frequency.

Key words: *vibration, rotary drier, frequency response*

1. Description of goals

The goal of vibration analysis of rotary drier developed by Bosch Siemens Hausgeraete, Michalovce was the evaluation of vibration transfer from motor to the bottom plate. Obtained results should be used as comparative values for experimental results from point of view of allowed level of vibration. To obtain physically relevant results for basic insight of its functional and vibrational properties 3D model of drier bottom plate (Fig. 1) includes bearings, transmission-device with belt and bottom plate with attachment elements.

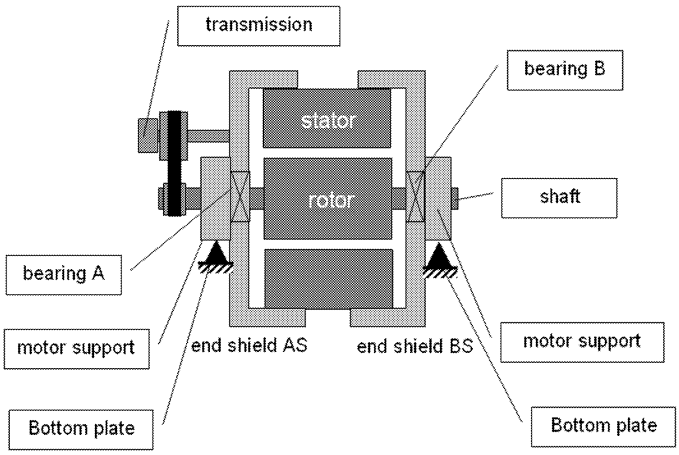

Fig.1: Scheme of drier's bottom plate

2. Task steps

The requested research oriented to the virtual dynamic analyses of mechanical system with gross motions dictates to adopt mechanical system simulation technology to perform

* Assoc. Prof. F. Palčák, Ph.D., MSc. M. Vančo, Strojnícka fakulta, Slovenská technická univerzita v Bratislave, Nám. slobody 17, 812 31 Bratislava

following task steps:

1. For dynamic simulation with 3D-Submodel of drier motor including bearing, transmission device and belt (without bottom plate) an unbalance of 200 mg on rotor (rotation 2730 rpm) and torsion of 100 Hz, 200 Hz and 300 Hz was used as dynamic load. The results were time dependent quantities on the outer ring of the bearing, side shields and stator (rigid bodies).
2. Vibration of the motor was investigated using MSC.ADAMS/Vibration. Obtained results contain frequency response functions from excitation point on motor to the outer ring, side shields and stator.
3. Based on the results form the first and second step a virtual numerical 3D-Model of drier bottom plate was developed. Time-domain dynamic analyses were used to verify functionality and proper behavior of model. The time dependent displacements, velocities and accelerations of the bearings outer rings, side shields and stator (rigid bodies) were obtained for simulations based on the same loading conditions as in step 1.
4. Final step was dedicated to analyze transfer of vibration from motor to defined points on bottom plate (Fig. 7). Excitation was caused by rotating unbalanced mass within the range from 0.1 Hz to 10000 Hz.

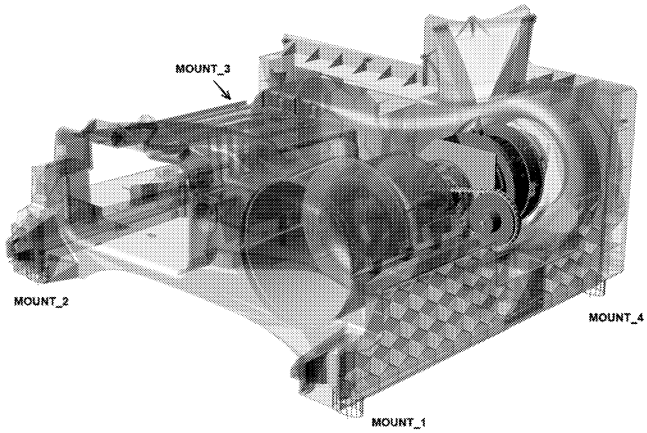

Fig.2: 3D model of drier bottom plate

3. Theoretical background of used computational technology

Vibration analysis is a frequency domain simulation of MSC.ADAMS models. This simulation can be a normal modes analysis in which the eigenvalues and mode shapes for the model are computed. The frequency domain simulation can also be a forced response analysis using the input and output channels along with the vibration actuators. Input channels provide a port into our system so we can obtain a plot of the frequency response or drive our system with an input force using a vibration actuator. When we create an input function a vibration actuator applies an input force to vibrate the system. A vibration actuator can contain expressions that let us use both time and frequency inputs. Each input channel must reference only one vibration actuator but each vibration actuator, however, can be associated with multiple input channels.

Swept sine defines a constant amplitude sine function being applied to the model.

$$f(\omega) = F\left[\cos(\theta) + \mathrm{j}\,\sin(\theta)\right] \tag{1}$$

where: f is the fequency ω dependet forcing function, F is the magnitude of the force and θ is the phase angle.

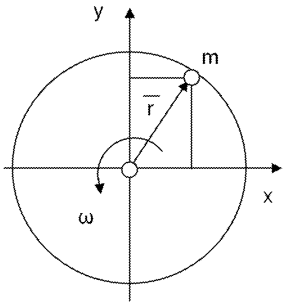

Fig.3: Principle of leading and lagging excitations

Transfer function is the magnitude and phase response produced by a given input channel at a given frequency ω for a given output channel.

For frequency response computation, the linearized model is represented as:

$$s\,\mathbf{x}(s) = \mathbf{A}\,\mathbf{x}(s) + \mathbf{B}\,\mathbf{u}(s)\ , \tag{2}$$

$$\mathbf{y}(s) = \mathbf{C}\,\mathbf{x}(s) + \mathbf{D}\,\mathbf{u}(s) \tag{3}$$

where: s is the Laplace variable and $\mathbf{A}$, $\mathbf{B}$, $\mathbf{C}$ and $\mathbf{D}$ are state matrices for the linearized model.

The system transfer function can be represented as:

$$\mathbf{H}(s) = \frac{\mathbf{y}(s)}{\mathbf{u}(s)} = \mathbf{C}(s\,\mathbf{I} - \mathbf{A})^{-1}\,\mathbf{B} + \mathbf{D} \tag{4}$$

where: $\mathbf{H}(s)$ is the transfer function for the model and $\mathbf{I}$ is the identity matrix of dimension equal to the number of system states.

For a given vibration analysis, the system frequency response $\mathbf{y}(s)$ is given as:

$$\mathbf{y}(s) = \mathbf{H}(s)\,\mathbf{u}(s)\ . \tag{5}$$

Modal coordinates are states in the frequency domain solution associated with a specific mode. Modes most active in a frequency response can be identified from the modal coordinates. The modal coordinates are computed as:

$$\mathbf{x}(s) = (s\,\mathbf{I} - \mathbf{A})^{-1}\,\mathbf{B}\,\mathbf{u}(s)\ . \tag{6}$$

PSD of output channels for given input PSDs is given as:

$$\mathbf{p}(s) = \mathbf{H}^{*}(s)\,\mathbf{U}(s)\,\mathbf{H}(s) \tag{7}$$

where: $\mathbf{p}(s)$ is the matrix of power spectral density, $\mathbf{H}^{*}(s)$ is the complex conjugate transpose of $\mathbf{H}(s)$ and $\mathbf{U}(s)$ is the matrix of input spectral density.

4. Modelling of contact forces

For models of contacts in our model were used 2D impact force contacts, which include the interaction between planar geometric elements (circle and point).

$$F_{\mathrm{n}} = k\left(g^{e}\right) + \mathrm{STEP}(g, 0, 0, d_{\max}, c_{\max})\,\frac{\mathrm{d}g}{\mathrm{d}t}\ . \tag{8}$$

In Eq. (8) g represents the penetration of one geometry into another, $\mathrm{d}g/\mathrm{d}t$ is the penetration velocity at the contact point, e is a positive real value denoting the force exponent, $d_{\max}$ is a positive real value specifying the boundary penetration to apply the maximum damping coefficient $c_{\max}$. The bearing model depicted on the Fig. 4 is advanced bearing model with possibility of ball settling and enabling to obtain relevant contact forces between inner ring and bearing ball (Fig. 5).

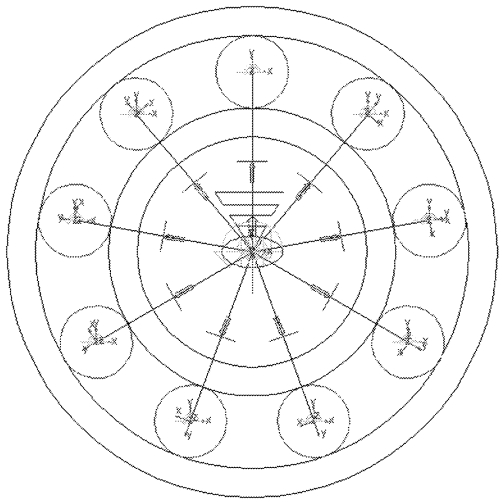

Fig.4: Advanced bearing model for contact forces and possibility of ball settling

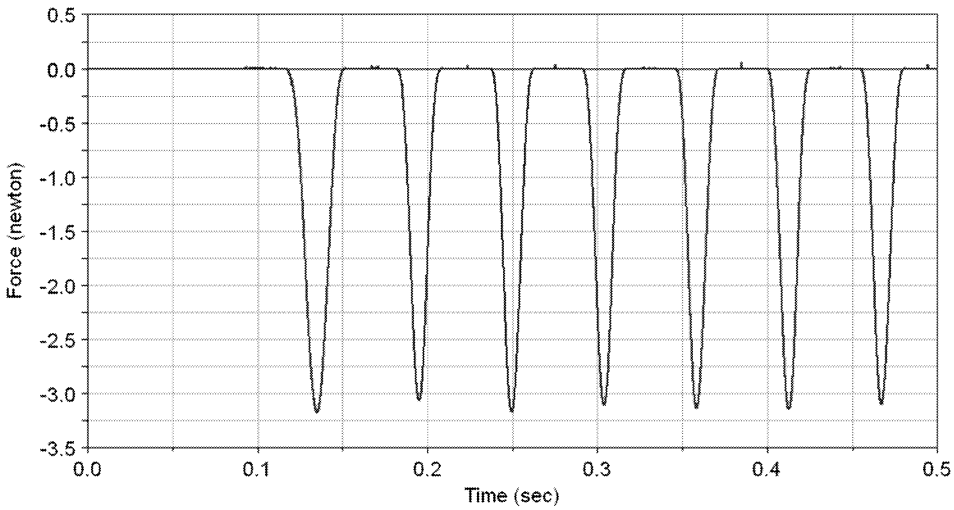

Fig.5: Time course of contact force between inner ring and bearing ball

On the Fig. 6 is comparison of time courses of response forces in fixed joint connecting bearing outer ring with ground with excitation from unbalanced mass and without excitation.

Idealized geometric constraints

To preserve guidance of belt against pulley and balls against rings in bearings there were used planar joints.

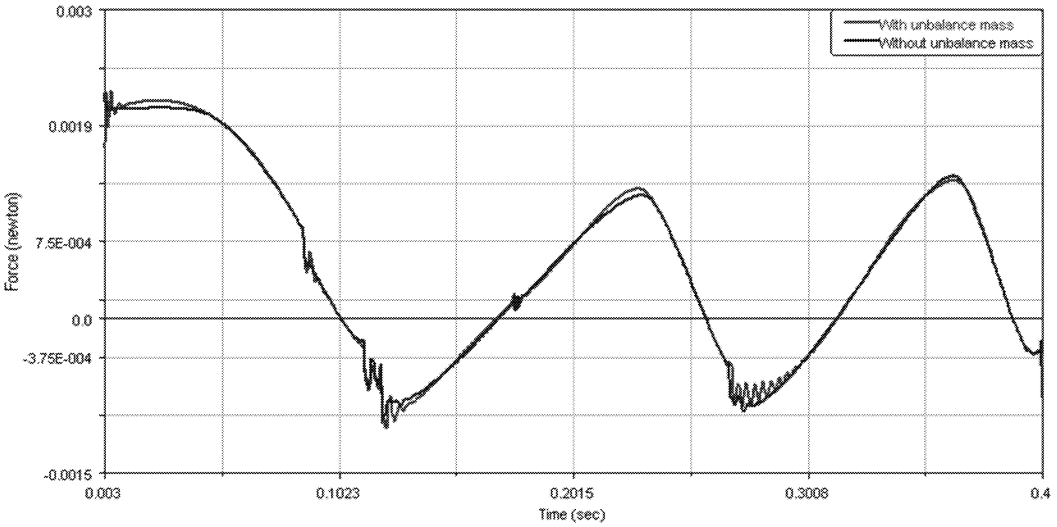

Fig.6: Time courses of response forces in fixed joint connecting bearing outer ring with ground; small wawes are caused by unbalanced mass

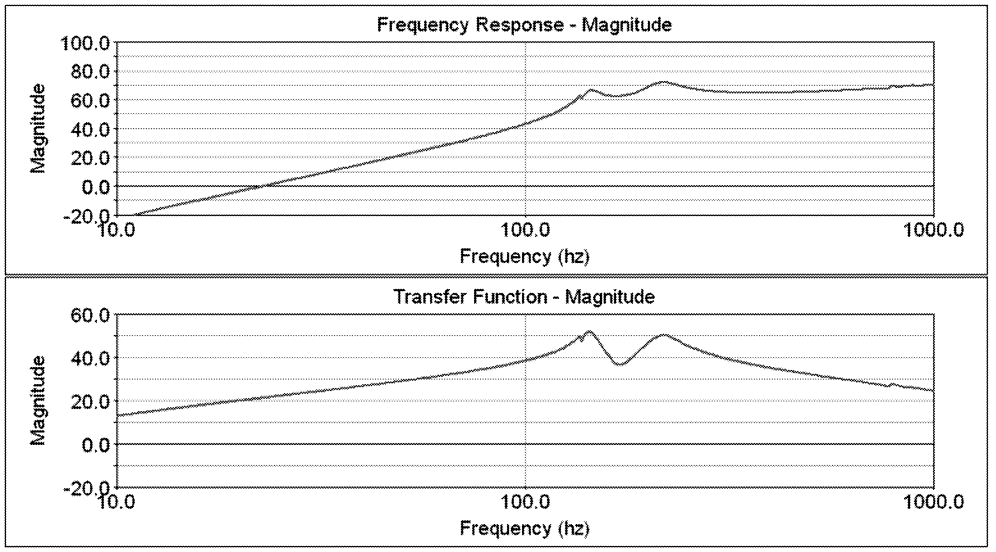

Fig.7: Frequency response function of AS shield acceleration and transfer function of AS shield acceleration

5. Disscusion of obtained results

On the Fig. 7 is frequency response function and transfer function corresponding to the excitation by unbalanced mass of 200 mg on the rotor.

On Fig. 8 is steady state portion of force response in attachment mount (MOUNT_1) after low pass filtering with cut off frequency 200 Hz because working range of drier is about excitation frequency 45.5 Hz.

On Fig. 9 is time range between 0.2 and 0.2219 corresponding to one revolution of motor shaft.

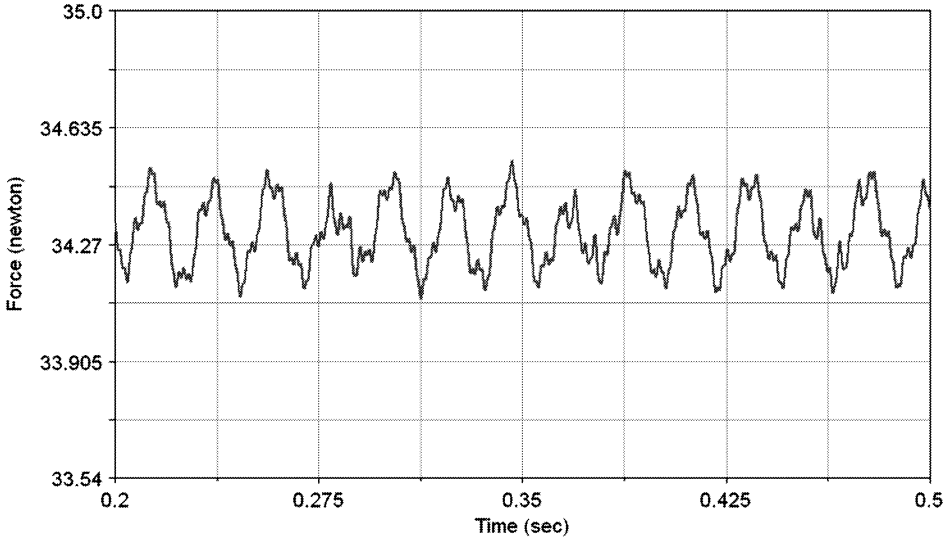

Fig.8: Force response in attachment mount (MOUNT_1 on Fig. 2) to the excitation from motor

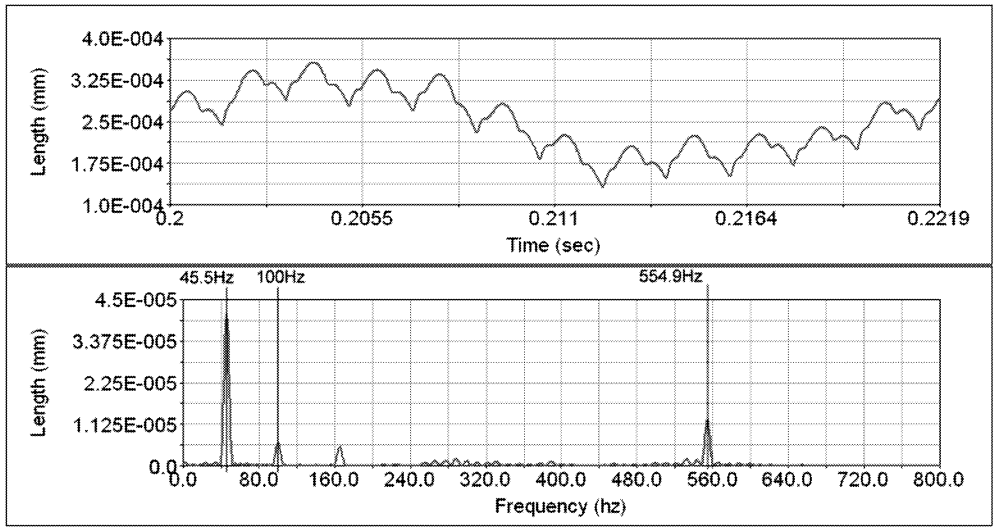

Fig.9: FFT analysis of displacement response of bottom plate in attachment mount (MOUNT_1)

From results yields that lower value (45.5 Hz) corresponding to rotation of unbalance mass and higher value (554.6 Hz) is caused by excitation due to contact of belt segments with pulley. In this section we deals with obtained frequency response functions (FRF from excitation point to the center of gravity of the outer ring, end shields, stator and bottom plate). Input point of excitation is located on the motor shaft. On the Fig. 10 is depicted the frequency response function of bottom plate center of mass acceleration.

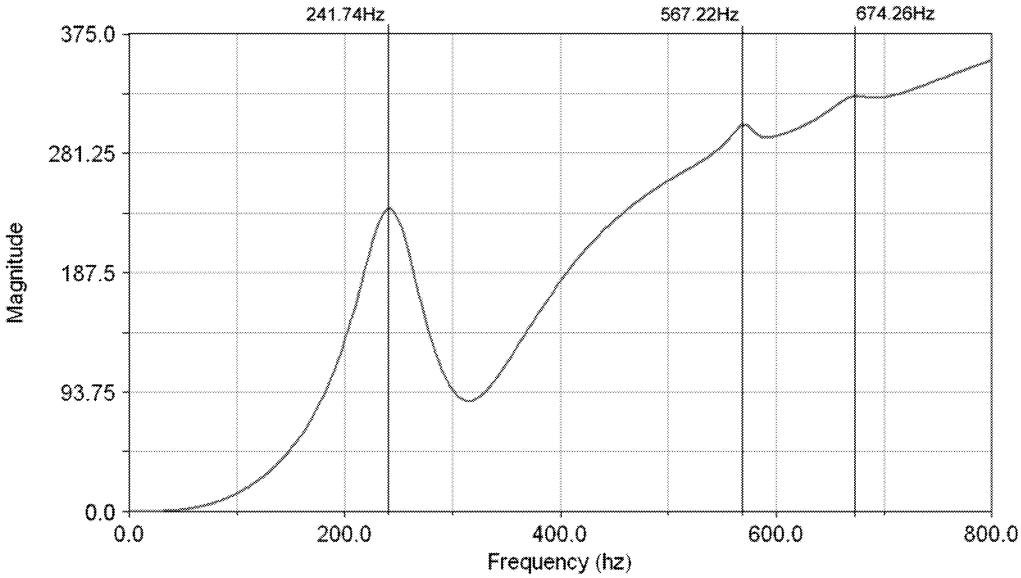

Fig.10: Frequency response function of bottom plate center of mass acceleration with frequency and magnitude axes in linear scale

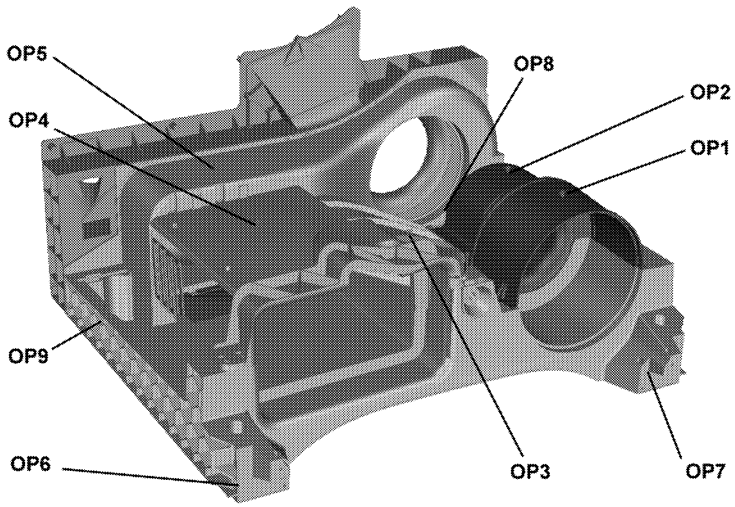

Fig.11: Position of output points for requested vibration responses

Other response outputs are denoted OP1–OP9 according to Fig. 11 with defined positions of output points. Output points OP6, OP7, OP8 and OP9 are on attachment mounts of bottom plate to the ground.

On figure Fig. 12 are results for acceleration of output points, because acceleration is often used as a measured quantity in real experiments. For comparison the frequency 357.73 Hz was selected, because in this value we can see amplification of responses.

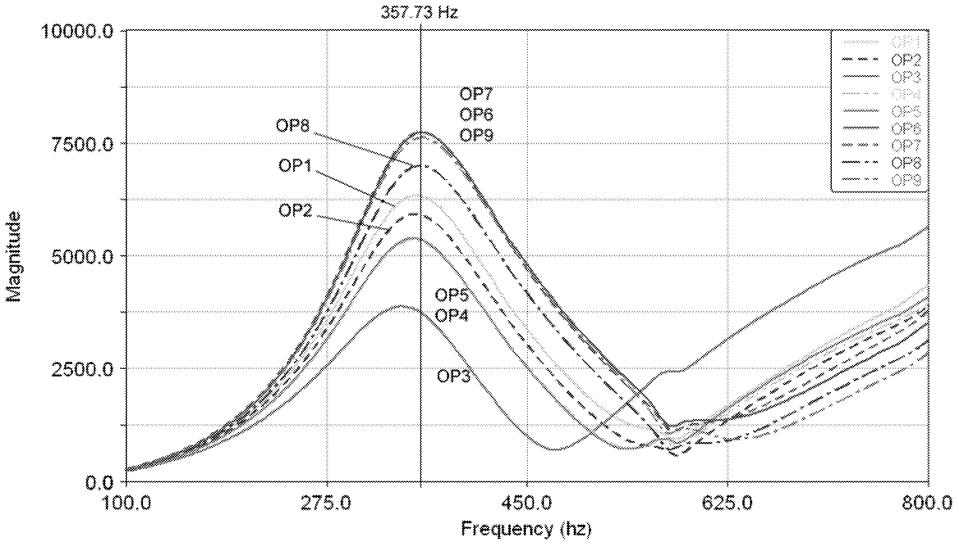

Fig.12: Frequency response functions for accelerations of bottom plate output points (frequency and magnitude axis are in linear scale)

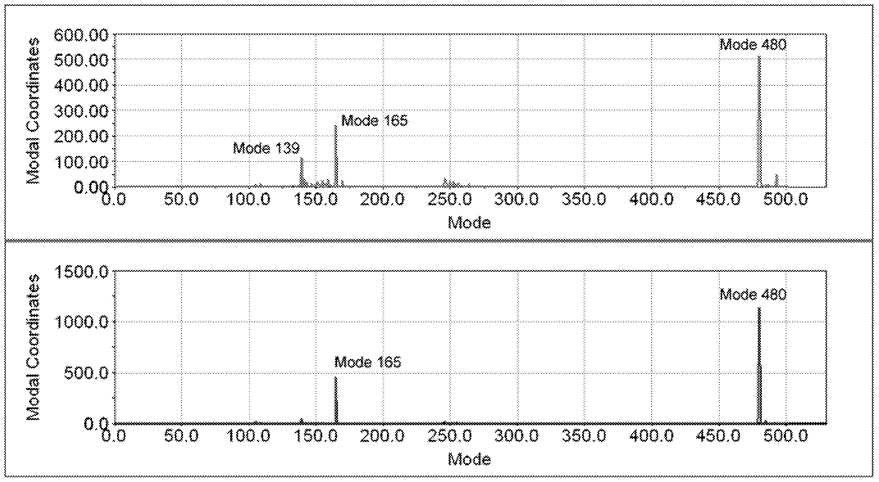

Fig.13: Modal coordinates corresponding to excitation frequency 45.5 Hz from input channel in horizontal (x-direction) are displayed in the upper plot, and from input channel in vertical (y-direction) are displayed in the lower plot

From whole frequency spectrum we concentrate on responses corresponding to the excitation frequency 45.5 Hz. On Fig. 13 we see which of normal modes (165, 480 in y-direction and 139, 165, 480 in x-direction) have highest values of modal coordinates. In Tab. 1 are sorted modal coordinates according to their magnitudes for excitation frequency (45.5 Hz) at input channel in horizontal x-direction, resp. vertical y-direction.

Input channel x-direction		Input channel y-direction	
Mode	Modal Coordinate	Mode	Modal Coordinate
480	0.358416	480	0.584575
165	0.168851	165	0.233424
139	0.079461	139	0.0257517
493	0.0335921	479	0.0218263
141	0.0224954	485	0.0155453
246	0.0220614	105	0.00755551
159	0.0191246	246	0.00744555
170	0.0186687	141	0.00726804
155	0.0184912	255	0.00697145
250	0.0157475	245	0.00660005

Tab.1: Modal coordinates for excitation frequency 45.5 Hz from input channel in horizontal x-direction, resp. vertical y-direction in the tabular form

6. Conclusion

To obtain better understanding of vibration transfer from motor to the bottom plate all three types of obtained results, from functional, time domain and frequency domain analyses were presented in this paper. It can be concluded, that all obtained results are acceptable from physical point of view and with respect to accuracy and performance are in line with expectations.

The FFT analysis of results from dynamic simulation of the motor in time domain confirmed correctness of the excitation frequency 45.5 Hz corresponding to the rotation 2730 rpm. In the first dynamic time domain simulation we detected unwanted influence of belt, which is documented by FFT analysis on Fig. 6 (frequency 554.6 Hz) corresponding to excitation of belt segments (for one revolution of shaft, 12.2 segments passes over shaft pulley and therefore $12.2 \cdot 45.5 = 555.1$). From Fig. 8 we can conclude that the highest values of acceleration are on attachments points of bottom plate to the ground (OP6, OP7, OP8 and OP9).

For documentation how is possible to obtain better insight into modal properties we prepared figures Fig. 9 with modal coordinates related to excitation frequency (45.5 Hz). The highest modal coordinates give us information which normal modes (165, 480 in y-direction and 139, 165, 480 in x-direction) contribute to unwanted frequency response.

As was stated, from methodical point of view the virtual model used for this research consist of rigid motor shaft and bottom plate with compliant attachments, which is initial phase of reality representation for study of vibration transfer to the bottom plate. The main goal in next steps of research will be to achieve properties of virtual 3D-model of drier bottom group closer to the reality. A necessary refining of the virtual 3D-model of bottom group should be achieved using input data obtained by physical experiments (nonlinear characteristics of compliant attachment elements). Further step of refining the rigid parts considered in the initial model (shaft, side shields, bottom plate) should be replaced by flexible bodies.

Acknowledgement

This work was supported by the Scientific Grant Agency of the Slovak Republic VEGA under the grant number 1/2092/05. This support is gratefully acknowledged.

References

[1] Harris C.M., Piersol A.G.: Harris' Shock and Vibration Handbook – Fifth Edition, McGraw-Hill, 2002
[2] Inman D.J.: Engineering Vibration, Prentice Hall, Inc., 2001
[3] Mathews C.: Engineers' Guide to Rotating Equipment, Professional Engineering Publishing Limited, 2002
[4] Mobley K.R.: Vibration Fundamentals, Newnes – Reed Elsevier Group, 1999

Received in editor's office: January 16, 2006
Approved for publishing: May 25, 2006

Note: The paper is an extended version of the contribution presented at the national conference with international participation *Engineering Mechanics 2005, Svratka, 2005.*